Recovery from monocular deprivation using binocular deprivation: Experimental observations and theoretical analysis

Brian Blais[1,3], Mikhail Frenkel[2], S. Kuindersma[1],
Rahmat Muhammad[2], Harel Z. Shouval[3,4], Leon N Cooper[3], Mark F. Bear[2]

[1]Department of Science and Technology
Bryant University, Smithfield RI

[2]Howard Hughes Medical Institute
The Picower Institute for Learning and Memory
Department of Brain and Cognitive Sciences
Massachusetts Institute of Technology, Cambridge MA

[3]Institute for Brain and Neural Systems
Brown University, Providence RI

[4]Department of Neurobiology and Anatomy
University of Texas Medical School at Houston, Houston TX

Running Head: How binocular deprivation restores visual responses

Corresponding Author: Mark Bear, mbear@mit.edu, Picower Institute for Learning and Memory, Massachusetts Institute of Technology, 77 Massachusetts Avenue, 46-3301, Cambridge, MA, 02139

Keywords: homosynaptic, long-term depression, ocular dominance plasticity, mouse visual cortex, BCM theory

Abstract

Ocular dominance (OD) plasticity is a robust paradigm for examining the functional consequences of synaptic plasticity. Previous experimental and theoretical results have shown that OD plasticity can be accounted for by known synaptic plasticity mechanisms, using the assumption that deprivation by lid suture eliminates spatial structure in the deprived channel. Here we show that in the mouse, recovery from monocular lid suture can be obtained by binocular lid suture but not by dark rearing. This poses a significant challenge to previous theoretical results. We therefore performed simulations with a natural input environment appropriate for mouse visual cortex. In contrast to previous work we assume that lid suture causes degradation but not elimination of spatial structure, whereas dark rearing produces elimination of spatial structure. We present experimental evidence that supports this assumption, measuring responses through sutured lids in the mouse. The change in assumptions about the input environment is sufficient to account for new experimental observations, while still accounting for previous experimental results.

INTRODUCTION

Ocular dominance (OD) plasticity in visual cortex is a powerful paradigm to investigate how experience and deprivation modify connections in the brain. In the classic experiments of Wiesel and Hubel, a rapid ocular dominance shift was achieved through the occlusion of one eye (Law et al. 1994; Wiesel and Hubel 1963). Monocular lid suture (MS) causes cortical neurons to lose responsiveness to the deprived eye by a process that is dependent on the structure of activity in the deprived eye (Blakemore 1976; Rittenhouse et al. 1999; Rittenhouse et al. 2006) not simply on the decrease in light-intensity. Various deprivation experiments that were traditionally performed in cats and have recently been replicated in rodents(Frenkel and Bear 2004; Mrsic-Flogel et al. 2007; Sawtell et al. 2003). Among other advantages, rodent visual cortex is amenable to chronic monitoring of the changes caused by deprivation. The results have challenged existing notions about the mechanisms responsible for deprivation.

We have previously shown that the BCM (Bienenstock et al. 1982) learning rule, implemented in simulations with patterned environments composed of natural images, can account for normal rearing and various deprivation experiments (Blais et al. 1999; Law et al. 1994). Modeling studies of ocular dominance plasticity were based on the assumption that inputs to the cortex from the deprived channel are active, but lack a spatial structure (*i.e.*, correlations). We have even been able to account for the difference between deprivation using MS and deprivation caused by a TTX injection into the eye (monocular inactivation, MI) (Frenkel and Bear 2004; Rittenhouse et al. 1999) simply by assuming that the activity in these different forms of deprivation has a different variance (Blais et al. 1999). Here we present experimental results in which a period of monocular deprivation is followed by either binocular lid suture (BS) or by placing the animals in the dark (DE). These two different variants produce significantly different experimental outcomes; a difference that cannot be explained by our previous assumptions.

In this paper we develop an input environment derived from natural images, with parameters appropriate for the mouse visual system. We alter our assumption about the impact of visual deprivation and assume that the input through a sutured eye preserves a degraded version of the structured patterned input (Krug et al. 2001). With these new assumptions we can account for these new experimental results, while still being able to account for previous experiments.

MATERIALS AND METHODS

Animal surgery and VEP recording

Animal surgery, visually evoked potential (VEP) recordings, and visual stimulation protocols were performed as previously described (Frenkel and Bear 2004; Frenkel et al. 2006; Sawtell et al. 2003). Briefly, a head post was attached to the skull and a recording electrode was implanted into layer 4 of the binocular zone of either the right or left primary visual cortex in mice at postnatal day 25 (P25). After at least 24-48 hrs of recovery, mice were habituated to a head restraint apparatus. Animals were placed in front of a computer monitor occupying their binocular visual field. VEPs in response to sinusoidal gratings of low spatial frequency (0.05 cycles/deg) square-reversing at 1 Hz were recorded on P28. Both contralateral and ipsilateral eye responses were collected. Subsequently the visual environment was altered for 3 to 7 days by performing one of the following procedures: monocular lid suture (MS), binocular lid suture (BS), monocular inactivation (MI) by intraocular TTX injections, or putting the animals into a light-tight room (dark exposure, DE). After 3-7 days, VEPs were recorded again in response to stimulation of contra- and ipsilateral eyes. In experiments to determine the effect of binocular lid closure on VEPs, baselines recordings were obtained using three spatial frequencies (0.05, 0.15, and 0.3 cycles/degree) with the eyes open. The animals were then anesthetized and the eyelids sutured. Following recovery from anesthesia, the VEPs were recorded again in response to the same stimuli with the eyes closed. At the end of all experiments, the animals were euthanized and the brains were processed for electrode placement verification. All animal procedures were done in accordance with the guidelines of MIT Animal Care and Use Committee.

Simulation training patterns

In order to approximate the mouse visual system, we start with the following basic properties of the retina, LGN and cortex. There is approximately 1000 photoreceptors feeding into 1 ganglion cell (Jeon et al. 1998; Sterling et al. 1988), and there is not much difference in cell density for mouse or cat retina. In both cat and mouse the retina/LGN responses show a center-surround organization, but with a center diameter around 7-10° for the mouse and less than 1° for cat (Grubb and Thompson 2003; Stone and Pinto 1993). Unlike the cat, the mouse has a functional contralateral bias on the order of ~2.5 to 1 (Drager and Olsen 1980; Frenkel and Bear 2004; Sawtell et al. 2003).

We use natural scene stimuli for the simulated inputs to the visual system. We start with images taken with a digital camera, with dimensions 1200 pixels by 1600 pixels and 40° by 60° real-

world angular dimensions (Fig 1A). We model the ganglion responses using a 32x32 pixel center-surround difference-of-Gaussians (DOG) filter to process the images, each pixel representing one photoreceptor. The center-surround radius ratio used for the ganglion cell is 1:3, with balanced excitatory and inhibitory regions and normalized Gaussian profiles. To correspond to the experimentally determined retinal properties, the images are rescaled before the DOG filter so that the center pixel size of the filter corresponds the real-world center size of 7° for the mouse. The original images are reduced to make each pixel correspond to their proper real-space size, and then the ganglion response filter is applied. We then include rotated versions of these filtered images, to make the environment more symmetric, and to eliminate any possible biasing effect of small numbers of patterns. The result is 3000 images, each of which has a size of 26x26 pixels. These images represent the ganglion cell responses during natural viewing. Figure 1A shows the original images, and the processed images that represent ganglion cell responses are shown in Figure 1B.

The specific biological details of the origin of the contralateral bias are not well known. To simply model the contralateral bias we assume that the measured responses ($r_{\text{contra-lateral}}$) are the combined responses of two populations of cells: purely binocular and purely monocular cells (Fig 1C). Thus, the contralateral responses arise as a mixture of both monocular and binocular cell responses, and the ipsilateral responses reflect binocular responses only.

$$r_{\text{contra-lateral}} = y_{\text{binocular-contra}} + y_{\text{monocular}}$$
$$r_{\text{ipsi-lateral}} = y_{\text{binocular-ipsi}}$$

where $y_{\text{binocular-contra}}$ is the response of binocular cells stimulated through the contralateral channel only, and $y_{\text{binocular-ipsi}}$ is the response of binocular cells stimulated through the ipsilateral channel only.

We assume that normally developed *binocular* cells have equal response to contra- versus ipsilateral stimulation ($y_{\text{binocular-contra}} \approx y_{\text{binocular-ipsi}}$), and further that under these circumstances the monocular and binocular cells contribute equally to the contralateral responses ($y_{\text{binocular-contra}} \approx y_{\text{monocular}}$). Thus, under normal conditions, the contralateral response will be approximately twice the ipsilateral response, giving rise to the roughly 2 to 1 ratio of contra- to ipsilateral responses (C/I ratio) observed experimentally. Changes to any of these details would not significantly affect the qualitative results presented here.

Synaptic Modification

We use a single neuron and the parabolic form of the BCM (Bienenstock et al. 1982) learning rule for

all of the simulations, where the synaptic modification depends on the postsynaptic activity, y, in the following way for a single neuron

$$\frac{dw_i}{dt} = \eta y\left(y - \theta_M\right)x_i$$
$$\theta_M \sim E_\tau\left[y^2\right]$$

where x_i is the ith presynaptic input, w_i is the ith synaptic weight, and y is the postsynaptic output activity. The constant, η, refers to the learning rate and the constant, τ, is what we call the memory constant and is related to the speed of the sliding threshold. For binocular cells, the input consists of contra- and ipsilateral presynaptic inputs. For monocular cells, there are only presynaptic inputs coming from the contralateral channel. The results are extremely robust to values of τ and η, which are generally chosen for practical, rather than theoretical, considerations. Each of these constants is related to the time-step for the simulations, but given the phenomenological nature of the BCM theory it is beyond the scope of this paper to make detailed comparisons between simulation time and real-time. Further, the fact that τ can be changed within a factor of 100 with no noticeable effect, the experiments presented here cannot be used address the time-scales of the molecular mechanisms underlying synaptic modification. All of the parameters and code for these simulations can be found on the project page for the simulation package *Plasticity* (http://plasticity.googlecode.com).

In the BCM learning rule, weights decrease if y is less than the modification threshold, θ_M, and increase if y is greater than the modification threshold. To stabilize learning, the modification threshold "slides" as a super-linear function of the output. The output, y, is related to the product of the inputs and the weights via a sigmoidal function, $y = \sigma(x \cdot w)$, which places constraints on the values of the output, keeping it in the range $-1 < y < 50$. The interpretation of negative values is consistent with previous work(Blais et al. 1998), where the activity values are measured *relative to spontaneous activity*. Thus, negative values are interpreted as activity below spontaneous. We continue this usage, in order to more easily compare with previous simulations. The role of the spontaneous level for the simulations in the natural image environment is discussed elsewhere (Blais et al. 1998).

The synaptic weights, and the modification threshold, are set to small random initial values at the beginning of a simulation. At each iteration, an input patch is generated from a combination natural

images and random noise, drawn from a zero-mean uniform distribution, and then presented to the neuron. The random noise is present to simulate the natural variation in responses of LGN neurons. Practically, it avoids the artificial situation of having mathematically identical inputs in the two input channels of the binocular cells. The exact values for the standard deviation of the noise in both the open- and closed-eye cases is shown in Table 1.

After each input patch is presented, the weights are modified using the output of the neuron, the input values and the current value of the modification threshold. This process yields orientation selective cells with the natural image environment (Blais et al. 1998). We then present test stimulus made from sine-gratings of 24 orientations, optimized for spatial frequency, and the response to the preferred orientation is selected as the neuron response. This is the response that is used in all of the plots. Simulations are ended when selectivity has been achieved and the responses are stable. Orientation tuning is calculated by taking the ratio of the first harmonic, F(1), of the Fast Fourier Transform (FFT) to the zeroeth harmonic, F(0).

Deprivation in the Mouse Visual System

In previous work with the BCM learning rule (Blais et al. 1999), deprivation was modeled using spatially uncorrelated noise in the deprived eye. This assumption has been shown to be necessary to be consistent with the experiments which demonstrate that presynaptic activity is needed for the ocular dominance shift in MS (Rittenhouse et al. 1999; Rittenhouse et al. 2006), and that *more* presynaptic activity in the deprived channel give rise to a *faster* ocular dominance shift. With BCM, the resulting ocular dominance shift in monocular deprivation occurs as a result of patterned input competing with unpatterned noise.

In the current work, we model inputs to the deprived channel as a significantly scaled-down and corrupted natural image stimulus, where the inputs are scaled down by a factor of 5 and corrupted with a Gaussian blur filter with additional random noise, again drawn from a zero-mean uniform distribution. This is to provide spatial structure to the deprived inputs in a simple and direct way, which is tunable and easy to interpret. Table 1 provides the exact parameters for the filter and the noise for deprived channels. The scaled-down factor of 5 is performed to be consistent with measurements through the lid-sutured eyes, shown in Fig 3. Thus, with the BCM learning rule and structure in the deprived channel, ocular dominance shifts in MS are a result of competition between two different qualities of patterned input: degraded versus normal patterns. BS effects are due to selective cells presented with degraded, noisy input patterns.

Results

Experimental observations of the effects of visual deprivation and recovery

In order to assess the effect of different deprivation protocols, we recorded VEPs (Sawtell et al. 2003) from young mice before and after the deprivation protocols. As shown previously (Frenkel and Bear 2004), 3 days of MS are sufficient to significantly reduce the magnitude of the VEP from the contralateral (C) eye, with no change in the ipsilateral (I) eye VEP (Fig 2A). The C/I VEP ratio shifts significantly, from approximately 2:1 to 1:1 ($P = 0.01$, Wilcoxon Signed Rank Test).

The loss of deprived eye responses reflects some form of competition, as demonstrated by a comparison of the effects of MS with a comparable period of binocular deprivation. Three days of BS causes no change in the magnitude of either the contralateral or ipsilateral eye VEP (Fig 2B). Similarly, 4 days of total light deprivation by DE has no effect on VEPs (Fig 2D).

If 3 days of MS are followed by 4 days BS, however, the result after these 7 days is indistinguishable from the initial condition at the first day of recording (Fig 2C). This implies that 4 days of BS produce a full recovery from prior MS. This result is surprising because, as seen above, BS alone does not seem to have any effect on cortical responses (Fig 2B). Some clues about why recovery from deprivation can occur during BS can be found in the surprising difference between BS and DE. When MS is followed by DE (Fig 2E) the ocular dominance shift is retained and is similar to the shift after MS alone.

The difference between MS followed by BS (Fig 2D) and MS followed by DE (Fig 2E) cannot be accounted for by our previous assumptions regarding normal and deprived rearing conditions. In particular our previous assumptions cannot account for the recovery of the deprived eye during the 4 days of BS. We postulate that these results can be accounted for by assuming that during an MS protocol, the activity pattern in the retina is not random noise, but that some patterned vision is preserved through the sutured eyelid (Krug et al. 2001). We examined this hypothesis in the awake mouse preparation by comparing VEPs evoked through open and closed eyelids. As expected, there was a significant (approximately 5-fold) decrease in VEP amplitude, but a response was still clearly evoked at low spatial frequencies (Fig. 3). We explore the concept of deprivation as degraded input using a model of synaptic modification in the mouse visual system.

Model of normal rearing

Our model of the mouse visual system and the training patterns appropriate for mouse simulations differ from assumption appropriate for cat simulations (Methods). First, the visual acuity in the mouse retina is much lower than for cat. This results in patterns of retinal activity in mouse (Fig 1B) that are blurry and carry little information about the high spatial frequency features of the visual environment. Second, the mouse has a significant contralateral bias. We represent this by assuming that half the cells in the mouse binocular region are binocular and respond equally to both eyes, while the other half is monocular and responds only to the contralateral eye (Fig 1C).

In Figure 4 we show the development of cortical responsiveness during normal rearing (NR) (Blais et al. 1998; Law et al. 1994). Normal rearing (NR) is modeled using inputs derived from natural images (Methods), the synapses are modified with the BCM learning rule (Methods), and the cell develops normal orientation-selective responses. On the left hand side of Fig 4A we show the maximal contralateral and ipsilateral responses to test stimuli as they develop over time in a binocular cell. The response to stimulation of both eyes is nearly identical. On the right hand side of Fig 4A we show the developing responses of a monocular cell. The cortical response shown in Fig 4B, is a sum of the responses of the monocular and binocular cells, as would be reflected in a population measure such as a VEP, and we see that it develops the observed contralateral bias.

This is the first time that images appropriate for the mouse visual systems acuity have been used for simulations of developing cortical receptive fields. Analogous to the development of receptive fields using higher acuity images, orientation selectivity is developed with lower acuity images, but cells are more broadly tuned and are tuned to lower spatial frequency (data not shown) as would be expected for the rodent visual system (Gordon and Stryker 1996; Metin et al. 1988).

Simulations of deprivation experiments and recovery

A major question posed by the experimental results of Figure 2, is why there is such a difference between MS followed by BS and MS followed by DE. In this paper we assume that these protocols differ in their input environment. We assume that in MS the input coming from the deprived eye is a significantly scaled-down and degraded version of the patterned input present in the non-deprived eye. Similarly, in BS input from both eyes is degraded. We implement the degradation by convolving the inputs with a Gaussian blur filter and adding random noise (see Methods section for details). In contrast we assume that during DE the activity in both channels is comprised entirely of random noise. Table 1 gives the properties of the pattern and noise in all of the deprivation protocols.

The simulated outcome of MS driven by degraded inputs (Fig 5A) appears no different from the

consequences deprivation resulting from uncorrelated noise. Despite the presence of structure in the retinal activity, the deprived contralateral eye is depressed, and the ratio between contra and ipsi responses (C/I) changes from 2 down to 1, as observed experimentally (Fig 2A). This occurs because the open eye input has more structure than the deprived eye input, and wins in the resulting competition between the two eyes. BCM theory has the property that there is competition between input patterns, with the neuron modifying its synapses to achieve maximal selectivity. As such, when the neuron is presented with an environment with 2 separate components, like the MS environment with degraded and non-degraded inputs, synapses will modify and the neuron will select the non-degraded inputs preferentially. Thus, the results of MS can be achieved with both degraded inputs or random noise in the deprived channel. However, as we show presently, the results of BS can be only achieved with degraded inputs.

Binocular suture (BS) following normal rearing appears to have little effect on absolute visual responsiveness (Fig 5B,C). However, a finer examination of the receptive fields shows us that they indeed change after BS (Fig 6A)—they lose selectivity and respond to optimally to lower spatial frequencies because they become sensitive to the degraded structure in the binocularly deprived channels. However when NR is followed by DE, the receptive fields do not change appreciably—they remain selective and responsive to the same optimal spatial frequency as normal mice (Fig 6B). This is one of the testable predictions of this model.

When 3 days of MS are followed by BS (Fig 5C), we obtain a full recovery of the deprived eye responses. This is consistent with experimental results (Fig 2D). In contrast, when MS is followed by DE no recovery occurs (Fig 5E) as observed experimentally. The recovery in the BS case occurs because the neuron retains the degraded structure in the deprived channels, in the absence of competition with a non-deprived channel. In contrast, during DE there is no structure in the deprived input, and therefore responses can not recover.

DISCUSSION

Previous studies demonstrated that the BCM rule trained with an input environment composed of natural images can account for many experimental results under normal and deprived rearing conditions (Blais et al. 1999; Law et al. 1994; Shouval et al. 2002). In these previous simulations we assumed that monocular lid suture can be represented by spatially uncorrelated random activity in the deprived channel. Here we present experimental results showing that BS results in recovery of the previously deprived eye, whereas MS followed by DE results in no recovery. These results are

inconsistent with our previous assumptions. We show that we can theoretically account for these new experimental results if we change our assumptions about inputs from a channel deprived by lid suture. Here we postulate that inputs from a lid sutured channel are drastically scaled-down and degraded versions of normal mouse vision, and this assumption is sufficient to account for the new experimental observations. This new assumption can account for the new experimental results for the following reason: If the degraded input is in competition with a channel with normal vision, it will lose out and there will be depression of the response from the deprived channel. However, during BS both channels are degraded, but have sufficient visual structure for developing responsive cells, and recovering from MS. During dark rearing, in contrast, the channels have no structure and no recovery from MS is obtained.

Structure, Noise, and BCM Modification

The BCM learning rule has the property that, all other things being equal, the output value is maintained when input magnitude is changed. Thus, when the patterned input intensity decreases, the weights increase "homeostatically" to maintain the output. Responses to test or probe stimuli, however, will then be increased relative to the responses before changing the input magnitude.

BCM has a second property that, for selective neurons, the output is inversely proportional to the number of patterns in the environment to which it is selective: neurons respond stronger to more rare patterns. One outcome of blurring is to make more patterns similar, which would make a neuron less selective, and drive the weights down. Thus, the more degraded the patterned input, the closer the dynamics will be to the results from previous studies (Blais et al. 1999; Law et al. 1994; Shouval et al. 2002) using only noise: ocular dominance shifts from monocular deprivation will be more pronounced, and responses will decrease for binocular deprivation.

A third property of BCM is that if there is noise in addition to pattern, increased noise decreases the weights, again to maintain the overall mean output value. This effect is more rapid with more noise, as explored previously (Blais et al. 1999).

These three properties of the BCM modification rule put constraints on the parameter values needed to be consistent with the observed dynamics of deprivation. In the case of BS, in order to get no change following normal rearing, and full recovery following brief MS, the noise level, amount of degradation of the input patterns, and the scale of the input patterns must be closely balanced. Thus, the experiments place constraints on the parameter values. Using the parameters that are consistent with BS, the other results presented follow.

Robustness of the simulations

The results presented are robust to certain changes in the parameters or architecture, and are sensitive to others. The sensitivity leads both to predictions and to a better understanding of the source of the results. Time parameters, such as the learning rate and the memory constant, are not critical to any of the results presented. The learning rate is chosen for the practical reason of making sure the simulations run in a reasonable amount of time. The memory constant can be changed by at least a factor of 100 with no effect whatsoever, however if it is set too high then the neuron will experience strong oscillations and never converge.

The particular model of the contralateral bias presented here is simplistic, but we do not believe that the results are qualitatively dependent on this choice. The exact nature and source of the contralateral bias is not well understood, so the simpler the model the better until we have data to constrain the model further.

The choice of image degradation, random noise in the deprived channel, and the scale of the deprived inputs are far more critical to these results, and they are linked. If, for example, one changes the distribution from a uniform distribution to a normal distribution for the noise, it would have a similar effect to increasing the magnitude of the noise. This would tend to drive a BCM neuron to lower responses in BS. To remain consistent with the present results, one would have to modify the image degradation to be less degraded or perhaps reduce the scale of the deprived inputs. The homeostatic properties of BCM would allow the neuron to maintain responses, as long as a balance in the input properties are maintained.

A recent study by Mrsic-Flogel et al. (2007) used two-photon calcium imaging to measure responses of neurons after MS and BS. They observe increases in responses of binocular neurons after BS, and increases in deprived-eye responses in neurons devoid of open-eye input in MS. They suggest that this finding is inconsistent with a Hebbian-type learning mechanism (BCM, specifically), and is only consistent with a general homeostatic process which preserves the net visual drive of each neuron. However, the homeostatic property of BCM, combined with the small amount of pattern present in deprived inputs, would account for the increases in deprived-eye responses they observe. On the other hand, the DE results presented here are inconsistent with the homeostatic model they propose. A homeostatic mechanism would predict *even more increases* in responses following DE compared with BS, which is not observed.

Origin of Structured Input

In these simulations we assume that a channel deprived by lid suture carries a diminished and degraded version of the patterned input, and that dark rearing leads to uncorrelated noise. It is clear from the difference between the experiments in which monocular deprivation is followed by BS or DE that lid suture deprivation is very different from light removal. The critical difference may be that enough light can enter through the sutured eyelid to evoke cortical responses, albeit weakly (Fig. 3). Of course, the "patterns" resulting from the light through the eyelid are certainly not equivalent to patterned input during normal vision. It is possible that the light intensity through the sutured lid generates activity that yields structure (correlations) either in the retina or the LGN. Another possibility is the recruitment of feedback from the cortex to LGN, which could influence the correlations in LGN neuronal firing, which could lead to correlated input back to the cortex. Each of these possibilities is testable, and should help us determine the critical properties of the visual system involved.

Future Directions

A more biophysical model may be necessary to get the detailed dynamics, but the simulations presented here already help us to determine the issues at hand. Some of the assumptions need to be explored both theoretically and experimentally. For example, the origin of the contralateral bias is not completely understood, and might play a significant role in the dynamics of deprivation, although the results presented here are robust to different models of the bias. Most importantly, it is a prediction of this model that the LGN activity during lid suture is more correlated than the activity during dark exposure. These correlations should be experimentally verifiable, and their source explored.

The mouse visual cortex has now become the standard model to study ocular dominance plasticity. Among numerous advantages, the absence ocular dominance columns and other types of cortical anisotropy make chronic recordings of response changes in awake animals feasible, yielding data on changes in absolute and relative visual responsiveness when visual experience is manipulated. Moreover, VEP recordings can be made from layer 4, where information from the two eyes first converges onto the same neurons. The relative simplicity of the mouse visual cortex and the ability to measure the dynamics of plasticity at thalamocortical synapses make this an excellent system to bring theoretical models into closer correspondence with biological reality.

Grants

This work is partially supported by the Collaborative Research in Computational Neuroscience (CRCNS) grant (NSF #0515285) from the National Science Foundation and by the National Eye Institute

References

Bienenstock EL, Cooper LN, and Munro PW. Theory for the development of neuron selectivity: orientation specificity and binocular interaction in visual cortex. *J Neurosci* 2: 32-48, 1982.

Blais BS, Intrator N, Shouval HZ, and Cooper LN. Receptive Field Formation in Natural Scene Environments. Comparison of Single-Cell Learning Rules. *Neural Comput* 10: 1797-1813, 1998.

Blais BS, Shouval HZ, and Cooper LN. The role of presynaptic activity in monocular deprivation: comparison of homosynaptic and heterosynaptic mechanisms. *Proc Natl Acad Sci U S A* 96: 1083-1087, 1999.

Blakemore C. The conditions required for the maintenance of binocularity in the kitten's visual cortex. *J Physiol* 261: 423-444, 1976.

Drager UC, and Olsen JF. Origins of crossed and uncrossed retinal projections in pigmented and albino mice. *J Comp Neurol* 191: 383-412, 1980.

Frenkel MY, and Bear MF. How monocular deprivation shifts ocular dominance in visual cortex of young mice. *Neuron* 44: 917-923, 2004.

Frenkel MY, Sawtell NB, Diogo AC, Yoon B, Neve RL, and Bear MF. Instructive effect of visual experience in mouse visual cortex. *Neuron* 51: 339-349, 2006.

Gordon JA, and Stryker MP. Experience-dependent plasticity of binocular responses in the primary visual cortex of the mouse. *J Neurosci* 16: 3274-3286, 1996.

Grubb MS, and Thompson ID. Quantitative characterization of visual response properties in the mouse dorsal lateral geniculate nucleus. *J Neurophysiol* 90: 3594-3607, 2003.

Jeon CJ, Strettoi E, and Masland RH. The major cell populations of the mouse retina. *J Neurosci* 18: 8936-8946, 1998.

Krug K, Akerman CJ, and Thompson ID. Responses of neurons in neonatal cortex and thalamus to patterned visual stimulation through the naturally closed lids. *J Neurophysiol* 85: 1436-1443, 2001.

Law CC, Bear MF, and Cooper LN. Role of the visual environment in the formation of receptive

fields according to the BCM theory. *Prog Brain Res* 102: 287-301, 1994.

Metin C, Godement P, and Imbert M. The primary visual cortex in the mouse: receptive field properties and functional organization. *Exp Brain Res* 69: 594-612, 1988.

Mrsic-Flogel TD, Hofer SB, Ohki K, Reid RC, Bonhoeffer T, and Hubener M. Homeostatic regulation of eye-specific responses in visual cortex during ocular dominance plasticity. *Neuron* 54: 961-972, 2007.

Rittenhouse CD, Shouval HZ, Paradiso MA, and Bear MF. Monocular deprivation induces homosynaptic long-term depression in visual cortex. *Nature* 397: 347-350, 1999.

Rittenhouse CD, Siegler BA, Voelker CC, Shouval HZ, Paradiso MA, and Bear MF. Stimulus for rapid ocular dominance plasticity in visual cortex. *J Neurophysiol* 95: 2947-2950, 2006.

Sawtell NB, Frenkel MY, Philpot BD, Nakazawa K, Tonegawa S, and Bear MF. NMDA receptor-dependent ocular dominance plasticity in adult visual cortex. *Neuron* 38: 977-985, 2003.

Shouval HZ, Castellani GC, Blais BS, Yeung LC, and Cooper LN. Converging evidence for a simplified biophysical model of synaptic plasticity. *Biol Cybern* 87: 383-391, 2002.

Sterling P, Freed MA, and Smith RG. Architecture of rod and cone circuits to the on-beta ganglion cell. *J Neurosci* 8: 623-642, 1988.

Stone C, and Pinto LH. Response properties of ganglion cells in the isolated mouse retina. *Vis Neurosci* 10: 31-39, 1993.

Wiesel TN, and Hubel DH. Single-Cell Responses in Striate Cortex of Kittens Deprived of Vision in One Eye. *J Neurophysiol* 26: 1003-1017, 1963.

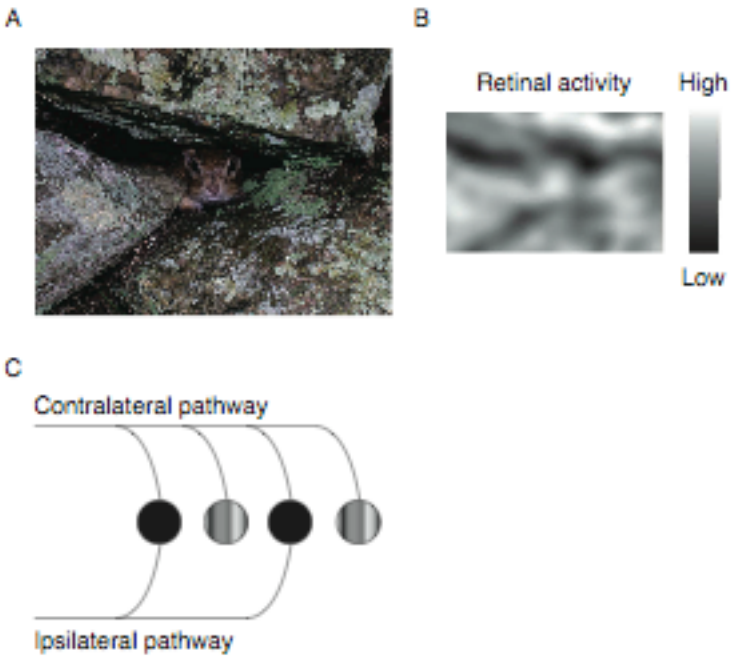

FIG. 1. Model assumptions, natural images and contralateral bias. Inputs that drive receptive field development as derived from natural images. A. An example of an original image. B. The resulting distribution of retinal ganglion cell and LGN neuron activity, using parameters appropriate for modeling the mouse visual system. The filter used is a difference-of-Gaussians (DOG) with a center/surround radius ratio of 1 to 3. C. The rodent visual system has a strong contralateral bias. We use a simplified architecture to model the contralateral bias. Two pools of cells combine to give responses. Binocular cells (black) respond equally to contra and ipsilateral stimulation, while monocular cells (gray) respond only to contralateral stimulation. If the number of binocular cells is equal to the number of monocular cells, then the contra-to-ipsilateral response ratio (C/I) will be ~2:1.

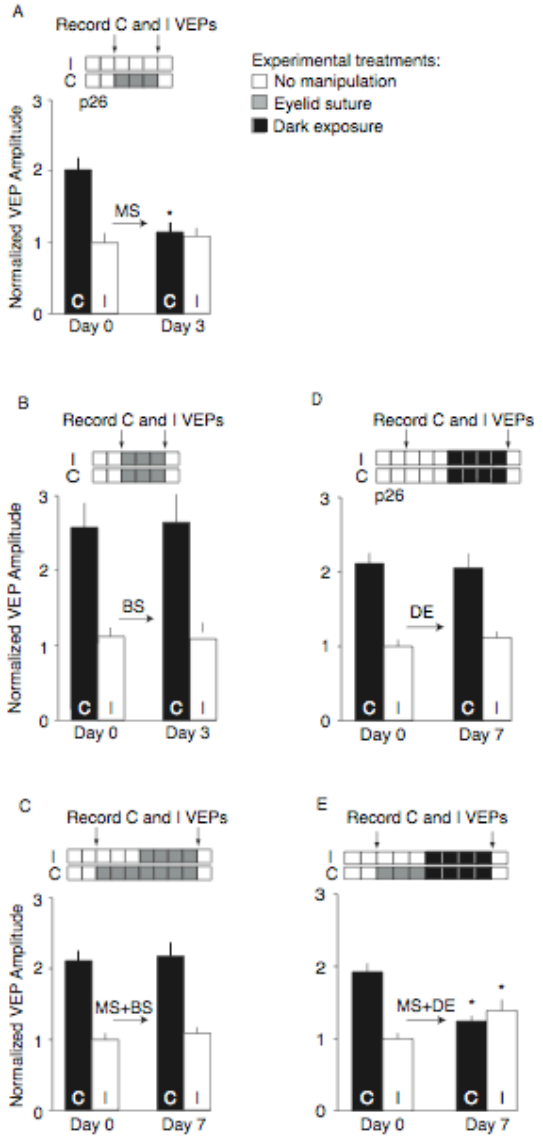

FIG. 2. Monocular deprivation and recovery: Experimental results. A. MS for 3 days causes depression of the contralateral VEP (n = 8, contralateral VEP amplitude ± SEM on day 0: 217 ± 18 μV; on day 3: 123 ± 15 μV; ipsilateral amplitude on day 0: 107 ± 14 μV; on day 3: 117 ± 12 μV, $P < 0.05$ paired t-test). B. BS for 3 days does not alter the VEPs (n = 6, contralateral VEP amplitude ± SEM on day 0: 222 ± 31 μV; on day 3: 227 ± 35 μV; ipsilateral amplitude on day 0: 87 ± 11 μV; on day 3: 92 ± 11 μV, data previously published by Frenkel and Bear, 2004). C. MS for 3 days followed by 4 days of BS produces responses at day 7 that are indistinguishable from responses at the beginning of the trial (n = 5, contralateral VEP amplitude ± SEM on day

0: 156 ± 10 μV; on day 7: 161 ± 14 μV; ipsilateral amplitude on day 0: 74 ± 6 μV; on day 7: 80 ± 7 μV). D. 4 days of DE do not change the VEPs (n = 6, contralateral VEP amplitude ± SEM on day 0: 148 ± 31 μV; on day 7: 144 ± 32 μV; ipsilateral amplitude on day 0: 70 ± 15 μV; on day 7: 78 ± 16 μV). E. 4 days of DE does not affect the shift caused by 3 days of MS (n = 10, contralateral VEP amplitude ± SEM on day 0: 144 ± 9 μV; on day 7: 92 ± 6 μV; ipsilateral amplitude on day 0: 74 ± 6 μV; on day 7: 104 ± 11 μV). Asterisks correspond to P-values less than 0.05 using paired t-test.

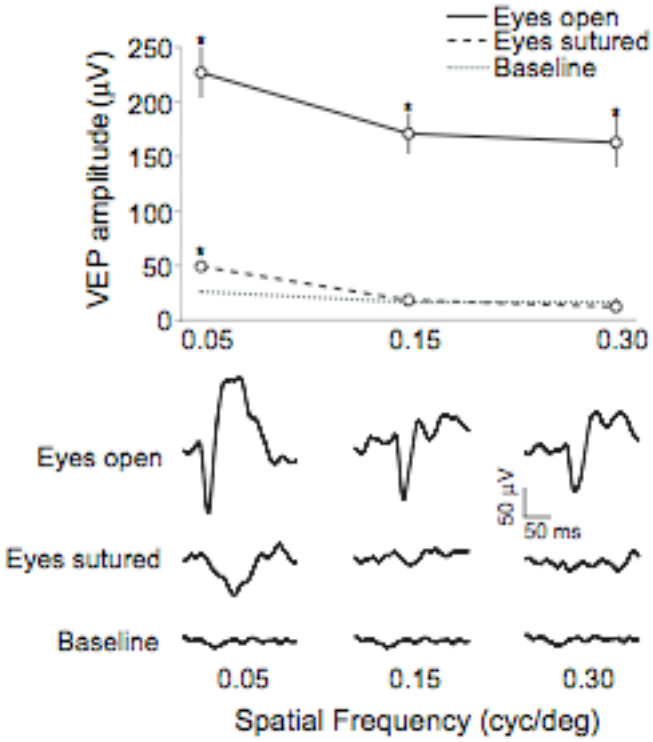

FIG. 3. VEP responses elicited through shut eyes. VEPs were recorded in response to grating stimuli of various spatial frequencies (0.05, 0.15, and 0.30 cyc/deg) at 100% contrast while both eyes were open (solid line) and following binocular deprivation by lid suture (black dashed line). Baseline recordings were made in response to a gray screen of equal luminance (gray dashed line). VEPs in response to all spatial frequencies were significantly greater than baseline when both eyes were open (post-hoc paired t-test, $p < 0.001$). Only the 0.05 cyc/deg grating stimulus was able to elicit a VEP response significantly different from baseline through the sutured eyes (post-hoc paired t-test, $p < 0.001$). Posthoc statistical comparisons were done after reaching significance with repeated measures two-way ANOVA ($p < 0.001$).

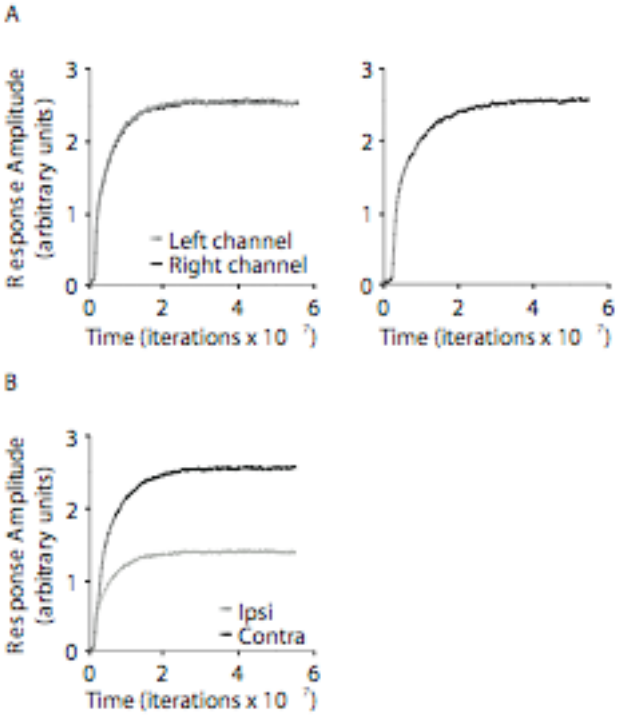

FIG. 4. Normal rearing in a mouse model. A. Binocular (left) and Monocular (right) cell responses, versus time. The y-axis represents the response of the trained neurons to test stimuli at the preferred orientation, measured in arbitrary units. As the model neuron is trained with natural images, the cell becomes selective, responding more strongly to oriented stimuli. B. Combining the binocular and monocular responses, to mimic the VEP recordings, yields contralateral and ipsilateral responses that are used for all of the simulations. The binocular and monocular cell responses contribute equally to the contralateral responses, and the ipsilateral responses include only binocular responses from the ipsilateral channel. All responses are measured in arbitrary units. Contra-to-ipsi response ratio (C/I) is approximately 2:1 for normal mouse.

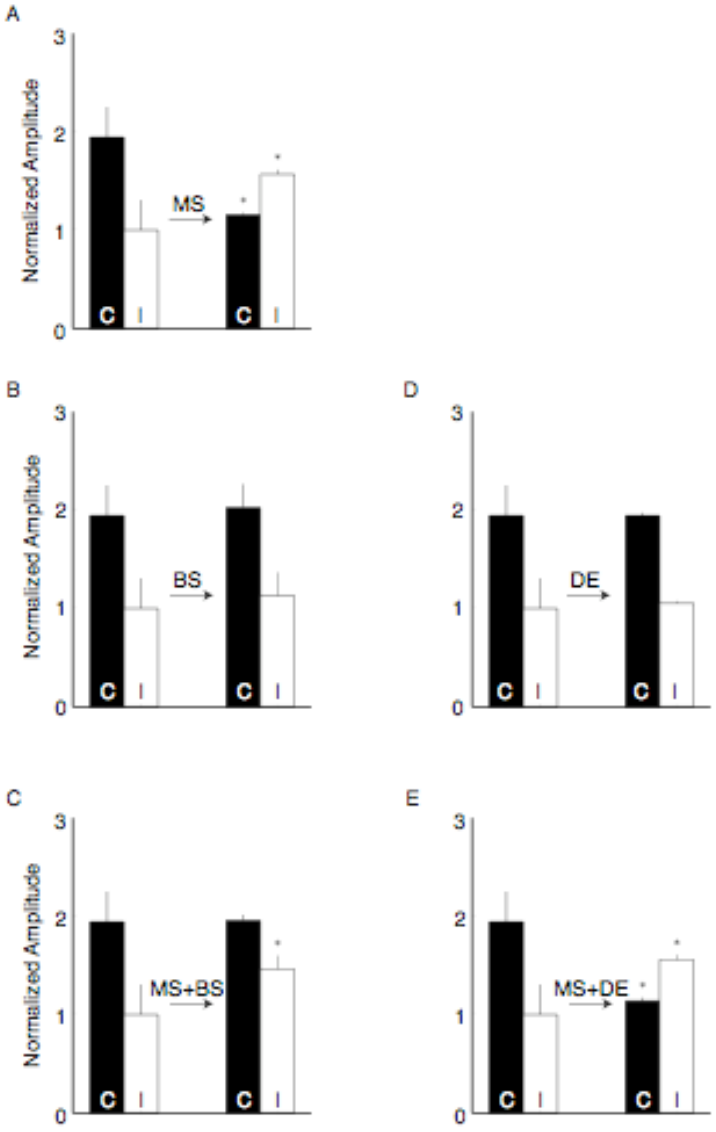

FIG. 5. Simulations of monocular deprivation and recovery. A. The contralateral bias is reduced during simulations of MS, in which the deprived channel is modeled as degraded and noisy patterned input. B. BS (two degraded channels) does not alter the contralateral bias or absolute responsiveness. C. BS after MS results in a recovery of the deprived eye responses. D. DE does not alter the contralateral bias or absolute responsiveness. E. DE after MS does not result in a recovery of deprived eye responses.

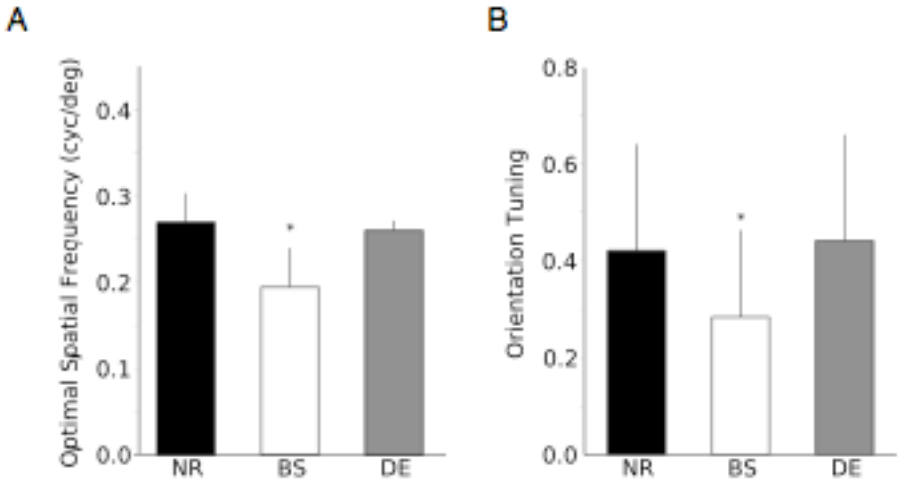

FIG. 6. Spatial frequency and orientation tuning of simulated cells after recovery. A. The optimal spatial frequency is reduced after BS, compared to normal cells. DE results in no change in optimal spatial frequency. B. Orientation tuning is reduced in BS and unchanged in DE compared to normal cells.

Default Parameters	
Parameter	**Value**
open-eye pattern standard deviation	1.0
deprived eye degraded pattern standard deviation	0.2
deprived eye degraded pattern blur size	3 pixels
open-eye noise standard deviation	0.1
deprived eye noise standard deviation	0.1
dark eye noise standard deviation	0.05
difference of Gaussian center/surround	2 pixel/6 pixel
total simulation time	$4 \cdot 10^{7}$ iterations
memory constant, τ	1000 iterations
learning rate, η	$5 \cdot 10^{-6}$ iterations^{-1}

Table 1: Default parameters for the simulations